AUGMENTATION OF FORCED FLOW BOILING HEAT TRANSFER BY INTRODUCING AIR FLOW INTO SUBCOOLED WATER FLOW

Y. KOIZUMI, H. OHTAKE, T. YUASA and N. MATSUSHITA

Department of Mechanical Engineering
Kogakuin University
2665-1, Nakano-machi, Hachioji-shi, Tokyo 192-0015, Japan

Phone: 81-426-28-4184, Fax.: 81-426-27-2360
E-mail: koizumiy@cc.kogakuin.ac.jp

Key words: Augmentation of heat transfer and CHF, Subcooled water and air mixture forced flow, Pump power

ABSTRACT

The effect of air injection into a subcooled water flow on boiling heat transfer and a critical heat flux (CHF) was examined experimentally. Experiments were conducted in the range of subcooling of 50 K, a superficial velocity of water and air $U_l = 0.17 \sim 3.4$ and $U_g = 0 \sim 15$ m/s, respectively. A test heat transfer surface was a 5 mm wide, 40 mm long and 0.5 mm thick stainless steel sheet embedded on the bottom wall of a 10 mm high and 20 mm wide rectangular flow channel. Nine times enhancement of the heat transfer coefficient in the non-boiling region was attained at the most by introducing an air flow into a water single-phase flow. The heat transfer improvement was prominent when the water flow rate was low and the air introduction was large. The present results of the non-boiling heat transfer were well correlated with the Lockhart-Martinelli parameter X_{tt}; $h_{TP}/h_{L0} = 5.0(1/X_{tt})^{0.5}$. The air introduction has some effect on the augmentation of heat transfer in the boiling region, however, the two-phase flow effect was little and the boiling was dominant in the fully developed boiling region. The CHF was improved a little by the air introduction in the high water flow region. However, that was rather greatly reduced in the low flow region. Even so, the general trend by the air introduction was that q_{CHF} increased as the air introduction was increased. The heat transfer augmentation in the non-boiling region was attained by less power increase than that in the case that only the water flow rate was increased. From the aspect of the power consumption and the heat transfer enhancement, the small air introduction in the low water flow rate region seemed more profitable, although the air introduction in the high water flow rate region and also the large air introduction were still effective in the augmentation of the heat transfer in the non-boiling region.

INTRODUCTION

The effect of gas phase introduction into a subcooled water flow on boiling heat transfer and a critical heat flux (CHF) was examined experimentally. This technique might be useful to get better heat transfer efficiency with less pump power. Thus, it has large possibility of application in wide industrial field. For example, air bubbling into water flow is possible way to manage to meet a sudden requirement for a high cooling rate in some emergency condition of nuclear reactors. It may of course be a reliable and economical way to limit the temperature increase of computer processing units.

Celata et al. [1] has reported that the boiling heat transfer coefficient is remarkably improved, approximately 10 times, by injecting air into a water flow. The liquid flow rate in their experiments was rather low. The injected air was not so much that the flow state observed in their experiments was a plug flow.

It is quite obvious that in the single-phase water flow, the high heat transfer coefficient and the high critical heat flux are obtained by increasing a mass flux. Thus, if air bubbling is coupled with increasing the mass flux, the heat transfer would be farther improved with less pump power increase.

In the previous paper [2], results of flow boiling heat transfer experiments of subcooled water and air mixture, conducted in the range of a superficial velocity of water and air U_l = 0.17 ~ 5.2 and U_g = 0 ~ 25 m/s, were reported. It was indicated that nine times enhancement of the heat transfer coefficient was attained at the most in the non-boiling region. The air introduction has some effect on the augmentation of heat transfer in the boiling region, however the two-phase flow effect was little in the fully developed subcooled-boiling region. As for the CHF, some improvement was perceived in the high mass flux region. However, it was rather reduced by the air injection in the low mass flux region.

In the present paper, new-updated data and results are presented and the power of a pump and a compressor required to flow water and air is discussed.

EXPERIMENTAL APPARATUS AND PROCEDURES

The schematic drawing of an experimental apparatus used in the present experiments is presented in Fig. 1. De-ionized water and air were used in the experiments. A test section was a rectangular flow channel of 20 mm wide and 10 mm high. The length was 830 mm. A heat transfer surface was a stainless steel sheet and the thickness, width and length were 0.2 mm, 5 mm and 40 mm, respectively. The heat transfer surface was embedded in the bottom wall of the flow channel flush to the surface of the wall at 450 mm from the inlet. A silicon resin sheet of 0.5 mm thick was glued with a silicon paste on the backside of the heat transfer surface to minimize heat loss from the back. Copper electrodes of 12 mm diameter were soldered at the both ends of the heat transfer surface.

Water pumped out from a water storage tank passes through flow meters, and then flows into the test flow channel through 150 mm mesh sintered metal plates mounted at the bottom and the top wall of the test section. Air supplied from a compressor through a flow meter flows into the inlet of the test section. A two-phase mixture of water and air flows in the test section and then out from the outlet of the test section. Air is discharged to atmosphere and water returns to the tank.

Low voltage DC current from an electric power supply system is provided to the electrodes of the heat transfer surface. The heat transfer surface is heated by Joule heating. A heat flux is derived from supplied DC current and voltage between the electrodes. Resistance of the electrodes and the solder are measured prior to each experiment and the

voltage drop due to these resistances is taken into account in calculating the heat flux. The current and the voltage are also utilized to derive the electric resistance of the heat transfer surface. Heat transfer surface temperature is obtained from the electric resistance by referring to the electric resistance dependency of the stainless steel on temperature. A flow state is pictured with a high speed and a usual CCD camera through view windows at the top and the side wall of the flow channel and recorded on video tape recorders.

The heat flux was increased stepwise in experiments. Measurement was performed after the facility was fully stabilized at each step. The heat flux was raised until the heat transfer surface physically burned out. The heat flux at the step right before the physical burn-out occurrence was defined as the CHF in the present experiments.

Subcooling of water at the inlet of the test section was set at 50 °C in all experiments. The experiments were conducted in the range of the water mass flux of 170 ~ 3400 kg/m^{2}s, the superficial velocity of air of 0 ~ 15 m/s and the heat flux of 0 ~ 8.0´ 10^3 kW/m^2. Bulk water was still subcooled at the outlet of the test section in the above experimental range. A flow state covered a dispersed-annular flow through a slug flow under the combination of the water and the air flow rate aforementioned according to the Baker chart [3].

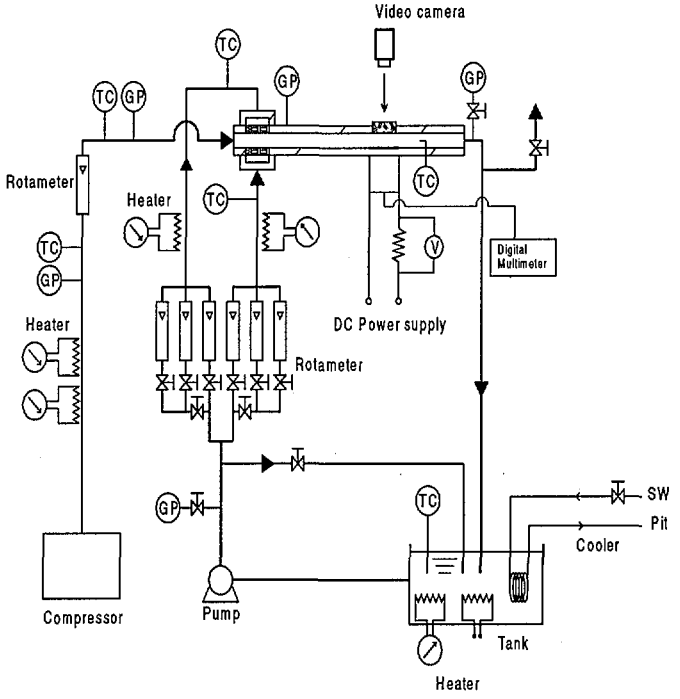

Fig. 1 Schematic of Experimental Apparatus

RESULTS AND DISCUSSIONS

Water Single-Phase Flow Heat Transfer

Measured heat transfer coefficients h_ls of the water single-phase flow in the non-boiling region are plotted in Fig. 2 in the form of Nusselt number $Nu = h_l D_{HY}/k_{lf}$ versus Reynolds number $Re = U_l D_{HY}/n_{lf}$. The heat transfer coefficients were calculated as $h_l = q/(T_W - T_l)$. Here,

D_{HY} denotes the hydraulic diameter, k the thermal conductivity, T the temperature, U the superficial velocity, n the kinematic viscosity, respectively. The subscripts l and w exhibit a water phase and a wall, and f expresses that the property is evaluated at the film temperature. The measured results are close to the correlation's values.

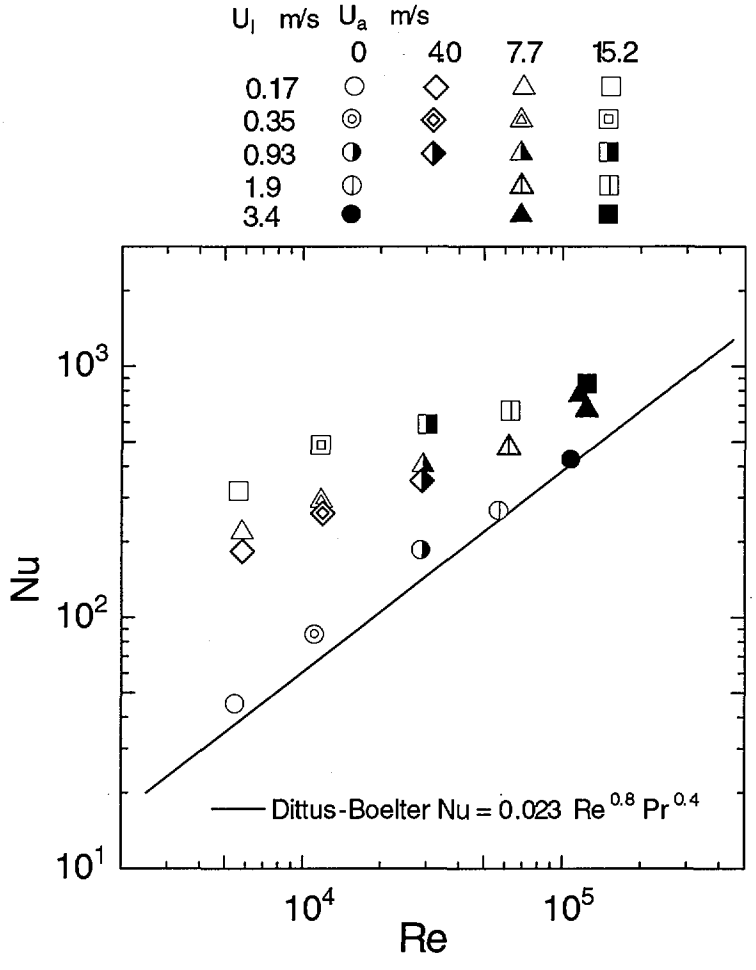

Fig. 2 Heat Transfer coefficient in the Non-Boiling Region

Boiling curves are presented in Fig. 3. Values of the Dittus-Boelter water single-phase flow heat transfer correlation, the Rohsenow [4] pool boiling heat transfer correlation with C_{sf} = 0.0132 which is the typical value for the stainless steel and the Thom et al. [3] and the Fujita et al. [5] subcooled-forced convection flow boiling heat transfer correlation are also delineated in the figure.

In Fig. 3, when the wall superheat DT_{sat} (i.e. the heat flux q) is low, the heat transfer is strongly affected by the flow rate. As the DT_{sat} is increased, the data plots become steep against the DT_{sat}. In the high wall superheat region, the results are close to values calculated by the Thom or the Rohsenow correlation. It is presumed that a heat transfer state there was fully developed boiling heat transfer. It was visually confirmed that intense boiling took place.

A final plot at the right end in each test condition in Fig. 3 expresses a CHF point. The CHF increases with an increase in the flow rate. When large bubbles agglomerate around the downstream end of the heat transfer surface, the burn-out occurred there.

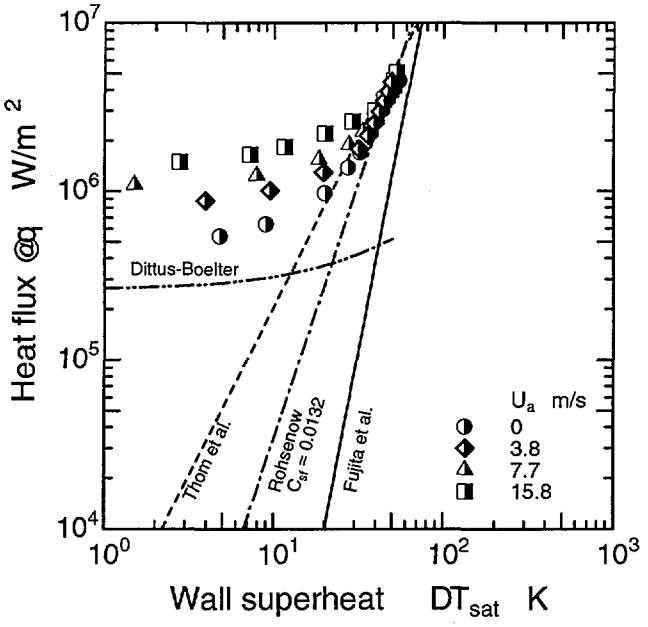

(a) Water Flow Rate U_l = 0.93 m/s

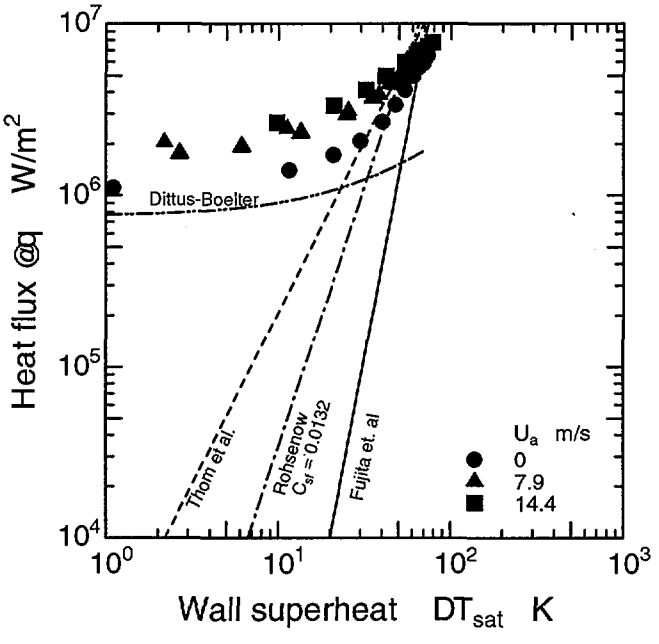

(b) Water Flow Rate U_l = 3.4 m/s

Fig. 3 Boiling Curve

Two-Phase Flow Heat Transfer

Results of the two-phase flow heat transfer are also included in Figs. 2 and 3. In the non-boiling region, the heat transfer coefficient is enhanced as the air flow is introduced. The larger the air introduction rate is, the higher the heat transfer coefficient is. The heat transfer coefficient is also augmented in the fully developed boiling region, however, the enhancement is small when the water flow rate was low. The CHF is elevated a little by the air introduction when the water rate is high. However, the CHF is decreased when the water flow rate is low. This will be further discussed in the following section.

The results of the two-phase flow heat transfer in the non-boiling region was analyzed considering that the flow condition of the air-water mixture two-phase flow was similar to what would appear in the one-component forced convection evaporation heat transfer. The Lockhart-Martinelli parameter X_{tt} for the turbulent-turbulent flow is usually defined as $1/X_{tt} = [x/(1-x)]^{0.9}(\rho_l/\rho_g)^{0.5}(\mu_g/\mu_l)^{0.1}$. The symbols x, mand r designate the quality, the viscosity and the density, respectively. The subscripts g and l stand for the gas and the liquid phase, respectively. In this definition, the viscosity and the density of air were used for μ_g and ρ_g in place of those of vapor. The quality was given as $x = G_a/(G_a + G_l)$, where G is the mass flow rate and the subscripts a and l exhibit air and water, respectively. Results so calculated are shown in Fig. 4. The symbol h is the heat transfer coefficient and the subscripts TP and L0 express the two-phase flow and the water single-phase flow, respectively. As for defining the Reynolds number, $Re = (\rho_a U_a + \rho_l U_l)D_{HY}/\nu_{lf}$.

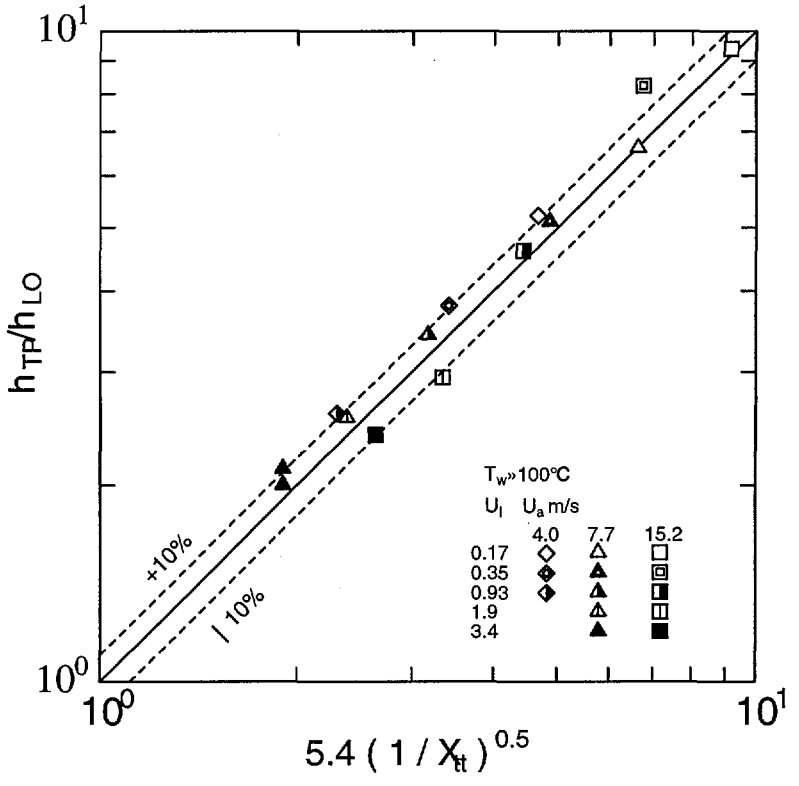

Fig. 4 Correlation of Heat Transfer Coefficient in the Non- Boiling Region

In Fig.4, the heat transfer coefficient is elevated approximately by 2 ~ 9 times by introducing air into the water flow. The two-phase flow effect is more prominent when the water flow rate is small and the air introduction is large. The present results are correlated as

$$\frac{h_{TP}}{h_{L0}} = 5.4\left(\frac{1}{X_{tt}}\right)^{0.50} \quad . \tag{1}$$

The RMS error of the equation is 10 %. Equation (1) is the same as the Dengler-Addoms correlation [3] except for the coefficient of 3.5.

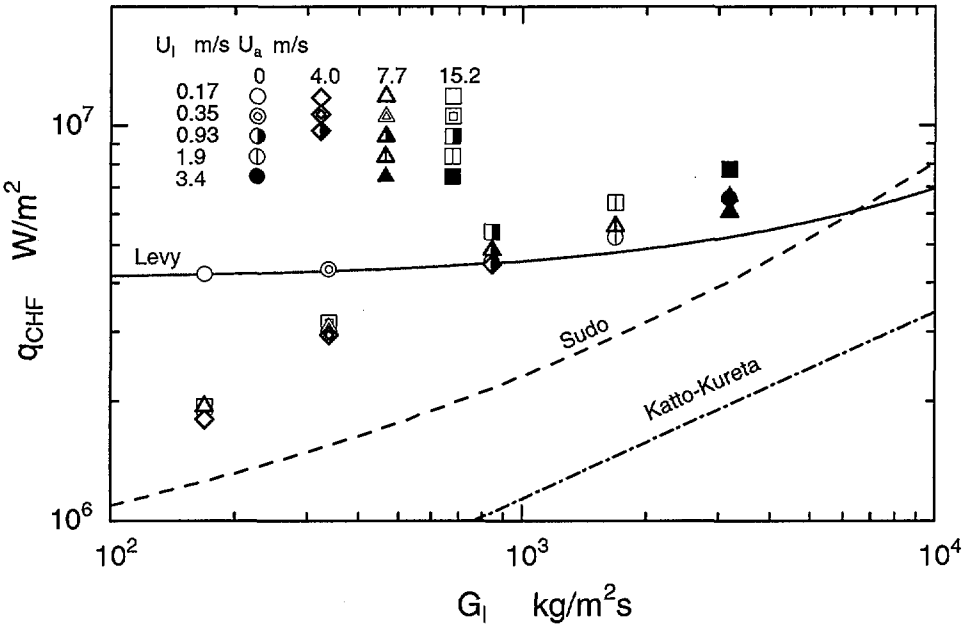

Fig. 5 Critical Heat Flux

Critical Heat Flux

Experimental values of q_{CHF} are plotted against the water mass flux in Fig. 5. q_{CHF}s predicted with the Katto-Kurata [6] correlation for the saturated forced convection flow boiling and the Sudo [7] and the Levy [8] correlation for the subcooled forced convection flow boiling are also included in the figure. The present experimental results of the subcooled single-phase flow are considerably larger than the predicted with the Katto-Kurata correlation and close to the predicted with the Levy correlation. The values of the Sudo correlation qualitatively agree with the experimental results at the high flow region.

When air is introduced in the high water flow region, the CHF is improved a little. However, the CHF is rather greatly reduced by the air injection in the low flow region. Even so, the general trend by the air introduction is that q_{CHF} increases as the air introduction is increased. Further examination is necessary.

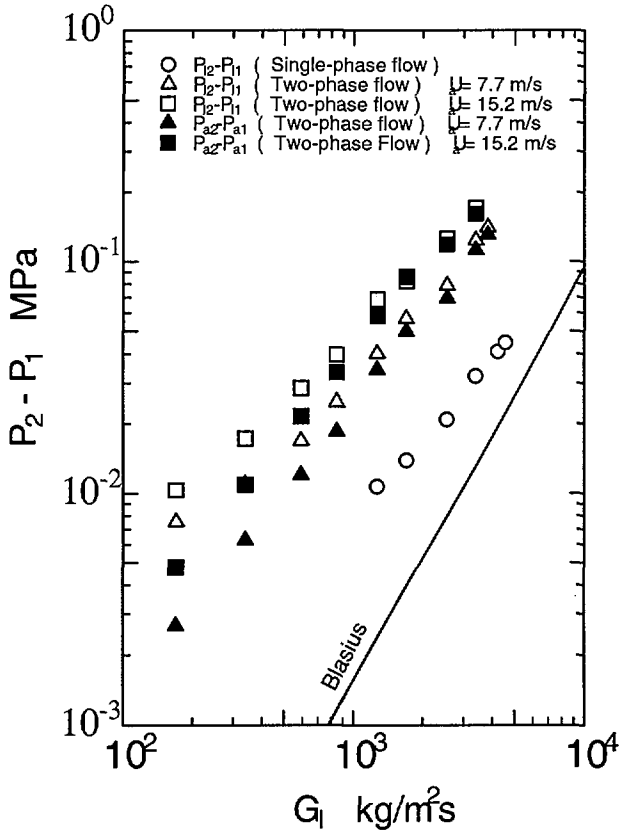

Fig. 6 Pressure Loss in the Test Section

Pump Power Economy By Two-Phase Flow Adoption

The pump power and the compressor power required are evaluated by using the pressure loss between the inlet and the outlet of the test section. The pump power is defined as

$$L_p = m_l v_l (P_{l2} - P_{l1}), \tag{2}$$

where m_l and v_l are the water mass flow rate and the water specific volume, respectively, and P_{l1} and P_{l2} are the water line pressure at the outlet and the inlet of the test section. Similarly, the compressor power is defined as

$$L_c = m_a (P_{a2} v_{a2} - P_{a1} v_{a1}), \tag{3}$$

where the symbol m denotes the mass flow rate, P the pressure and v the specific volume. The subscripts a, 1 and 2 express air, the outlet and the inlet, respectively. It should be noted that the real pump and the compressor power are a little bit different from Eqs. (2) and (3) since there exists pressure loss in piping from the pump or the compressor to the test section inlet.

The pressure losses measured are presented in Fig. 6. In the figure, calculated values

with the Blasius correlation are also included for comparison. As a matter of course, the pressure loss increases as air is introduced.

The total power of the pump and the compressor so calculated are plotted against the water mass flow rate in Fig. 7. According to the Dittus-Boelter correlation, the single-phase flow heat transfer coefficient is proportional to the 0.8th power of the mass flux. For example, at the point a in the figure, the heat transfer coefficient in the nonboiling region is increased by 7.0 times by introducing air into the water flow. If that improvement is performed by only increasing the water flow rate, the flow rate should be increased by 11.4 times. The pump power required then is exhibited by a' in the figure. It is obvious from the figure that the same improvement in the heat transfer is attained by less power increase in the air introduction case than in the single-phase flow case. The same situations are designated in the figure by without- and with-prime symbols.

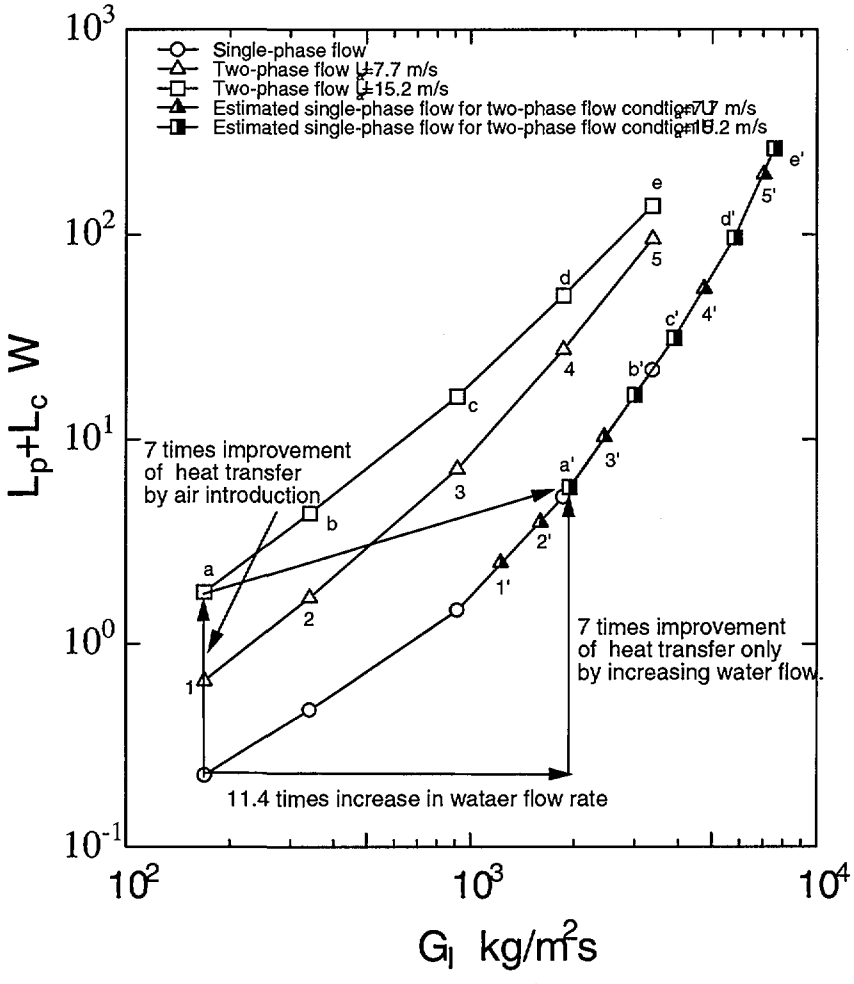

Fig. 7 Relation between the Pump and the Compressor Power and the Water Flow Rate

The benefit of the power in adopting the air introduction mentioned above is more clearly depicted in Fig. 8 where the heat transfer coefficients in the non-boiling region are plotted against the total power. The heat transfer is considerably enhanced by introducing air under the same power for circulating coolant.

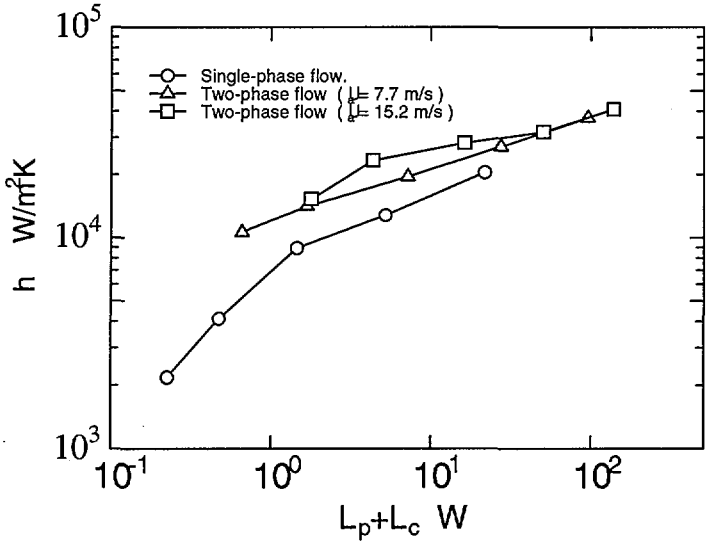

Fig. 8 Relation between the Heat Transfer Coefficient in the Non- Boiling Region and the Pump and the Compressor Power

The relation between a power ratio = $L_{single}/L_{two\text{-}phase}$, where

L_{single} : the water pump power to get the same heat transfer coefficient as that in the two-phase flow case by the single phase flow

$L_{two\text{-}phase}$: the total power of the pump and the compressor in the air introduction case and the heat transfer coefficient in the non-boiling region is illustrated in Fig.9.It is realized that the small air introduction in the low water flow rate region is more profitable, although the air introduction at the high water flow rate region and also the large air introduction are still effective in the augmentation of the heat transfer in the non-boiling region.

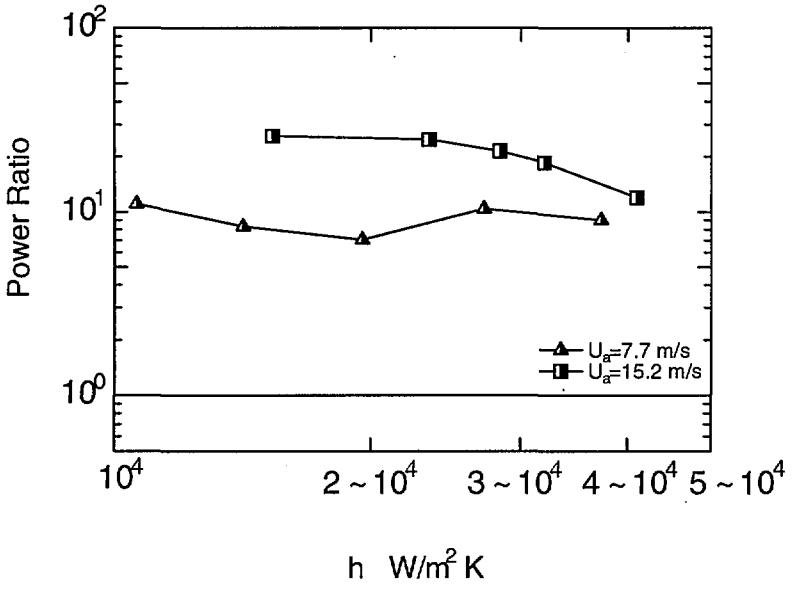

Fig. 9 Power Reduction Ratio by Air Introduction

CONCLUSIONS

The enhancement of heat transfer by the high mass flux, subcooled air-water two-phase flow was examined. Following conclusions were obtained.

(1) Nine times enhancement of the heat transfer coefficient in the non-boiling region was attained at the most by introducing the air flow into the water single-phase flow. The heat transfer improvement was prominent when the water flow rate was low and the air introduction was large. The present results of the non-boiling heat transfer were well correlated with the Lockhart-Martinelli parameter X_{tt}. The correlation obtained was the same form as the Dengler-Addoms correlation for the forced convection evaporation except for that the coefficient was 54 % larger.

(2) The air introduction to the subcooled water flow had some effect on the augmentation of heat transfer in the boiling region, however, the two-phase flow effect was small and the boiling was dominant in the fully developed boiling region.

(3) When air was introduced in the high water flow region, the CHF was improved a little. However, the CHF was rather greatly reduced by the air injection in the low flow region. Even so, the general trend by the air introduction was that q_{CHF} increased as the air introduction was increased. Further examination is necessary.

(4) When air was injected into a water flow, the heat transfer augmentation in the non-boiling region was attained by less power increase than that in the case that only the water flow rate was increased. From the aspect of the power consumption and the heat transfer enhancement, the small air introduction in the low water flow rate region was more profitable, although the air introduction in the high water flow rate region and also the large air introduction were still effective in some degree in the augmentation of the heat transfer in the non-boiling region.

REFERENCES

1. Celata, G. P., et al., Heat Transfer Enhancement by Air Injection in Upward Heated Mixed-Convection Flow of Water, Int. J. Multiphase Flow, 25(1999), 1033-1055.
2. Koizumi, Y., et al., Boiling Heat Transfer and CHF of Forced Flow of Subcooled Water and Air Mixture, Proceedings of 4th JSME-KSME Thermal Engineering Conference Vol. 1(2000), 1-445 – 1-449.
3. Ueda, T., Gas-Liquid Two-Phase Flow, Flow and Heat Transfer, Yokendo Co.(1981), 11-13, 259-265.
4. Rohsenow, W. M., A Method of Correlating Heat Transfer Data for Surface Boiling of Liquids, Trans. ASME, 74(1952), 969-976.
5. Fujita, Y, et al., Enhancement of Flow Boiling of Subcooled Water on Transverse Ribbed Surface, 5th ASME-JSME Joint Thermal Engineering Conference(1999), AJTE99-6365.
6. Katto, Y, and Kurata, C., Critical Heat Flux of Saturated Convective Boiling on Uniformly Heated Plates in a Parallel Flow, Int. J. Multiphase Flow, 6(1980), 575-582.
7. Sudo, Y., Critical Heat Flux of High-Subcooled High Mass Flux Flow at Atmospheric Pressure, Trans. JSME, 62-601B(1996), 148-154.
8. Levy, S., Prediction of the Critical Heat Flux in Forced Convection Flow, General Electric, GEAP-3961(1962).

NOMENCLATURE

C_{sf} Constants in the Rohsenow pool boiling correlation,

non-dimensional

D_{HY} Hydraulic diameter, m

G Mass velocity, kg/m^2s

h Heat transfer coefficient, W/m^2K

k Thermal conductivity, W/mK

L Power, W

m Mass flow rate, kg/s

Nu Nusselt number, h_lD_{HY}/k_{lf}, non-dimensional

P Pressure, Pa

q Heat flux, W/m^2

Re Reynolds number, U_lD_{HY}/n_{lf}, non-dimensional

v Specific volume, m^3/kg

T Temperature, K

U Superficial velocity, m/s

X_{tt} Lockhart-Martinelli parameter for turbulent-turbulent flow, $[(1-x)/x]^{0.9}(r_g/r_l)^{0.5}(m_l/m_g)^{0.1}$, non-dimensional

x Quality, non-dimensional

Greek Symbols

m Viscosity, Ns/m^2

n Kinematic viscosity, m^2/s

r Density, kg/m^3

Subscripts

1 Outlet

2 Inlet

a Air phase

b Evaluated at the bulk temperature

c Compressor

CHF Critical heat flux condition

f Evaluated at the film temperature

g Gas phase

l Liquid

p Pump

single Single-phase flow

two-phase Two-phase flow